$\pi^0\gamma$ invariant mass distribution in the low-energy $\gamma p \to \omega p$ reaction

Swapan Das
Nuclear Physics Division, Bhabha Atomic Research Centre, Mumbai-400085, India
(Received 7 January 2008; revised manuscript received 1 October 2008; published 31 October 2008)

The reaction mechanism for the correlated $\pi^0\gamma$ emission in the photon-induced reaction on a proton target is studied. Since this reaction is studied in the GeV region, one can assume that it proceeds through the formation of the vector meson in the intermediate state. The vector meson, being an unstable particle, decays into $\pi^0\gamma$ bosons after propagating a certain distance. The analysis shows that the $\pi^0\gamma$ event seen in coincidence in the final state dominantly arises owing to the decay of ω meson. The calculated results reproduce the measured $\pi^0\gamma$ invariant mass distribution spectra very well.

DOI: 10.1103/PhysRevC.78.045210 PACS number(s): 25.20.Lj, 13.75.Cs, 13.75.Gx

I. INTRODUCTION

Vector meson production in nuclear and particle reactions has opened up various avenues, providing ample opportunities for learning many interesting topics in physics. The leptoproduction of the vector meson is a potential tool for investigating the hadron structure of the photon [1]. Dilepton production in the intermediate-energy region is undoubtedly understood by the decay and interference of the vector mesons [1]. Since the vector meson strongly couples to the nucleon and its resonances [2,3], the dynamics of these resonances can be explored by studying the vector meson production process. In fact, there are predictions of many nucleonic resonances (see Ref. [4] and references their in), which are yet to be found. Vector meson production could be a useful probe to search for these missing resonances. It should be added that the subthreshold production of the vector meson can probe the low-lying resonances, such as $N(1520)$ [5].

In recent years, the production of vector mesons in nuclear reactions has drawn considerable attention for exploring its properties in the nuclear medium [6,7]. Indeed, it is a fundamental issue in nuclear physics. In this context, the $\pi^0\gamma$ invariant mass distribution spectrum was measured, in the recent past, by the CBELSA/TAPS Collaboration at the electron stretcher accelerator (ELSA) in Bonn [8] to look for the medium modification on the ω meson in the Nb nucleus. They have also taken data for this spectrum from the γp reaction. Here, we present the reaction mechanism for the $(\gamma, \pi^0\gamma)$ reaction on a proton target in the GeV region. In this energy region, the $\pi^0\gamma$ in the final state (according to the Particle Data Group [9]) can arise from the decay of low-lying vector mesons, such as $\rho^0(768)$, $\omega(782)$, and $\phi(1020)$. Therefore, I consider that this reaction proceeds through three steps: (i) the formation of vector mesons, (ii) the propagation of these vector mesons, and (iii) the decay of these mesons into the $\pi^0\gamma$ channel. Symbolically, this reaction goes as $\gamma p \to Vp; V \to \pi^0\gamma$, where V stands for the aforementioned vector mesons (i.e., $V \equiv \rho^0, \omega$ and ϕ).

The qualitative comparison (presented in the following) amongst the ρ^0, ω and ϕ mesons' contributions to this reaction shows that the ω meson contributes dominantly to this reaction. The data on the γp reaction show that the production cross section for the ρ^0 meson is the largest compared to those for the other two vector mesons in the energy region considered here. For example, the measured cross sections at 1.5 GeV beam energy, as reported by various group, are $\sigma_t(\gamma p \to \rho^0 p) \simeq 23\ \mu$b [10], $\sigma_t(\gamma p \to \omega p) \simeq 6.51\ \mu$b [11], and $\sigma_t(\gamma p \to \phi p) \simeq 0.17\ \mu$b [12]. Therefore, the measured $\sigma_t(\gamma p \to \rho^0 p)$ is about 3.53 times larger than the measured $\sigma_t(\gamma p \to \omega p)$, and the former is about 135.29 times larger than the measured $\sigma_t(\gamma p \to \phi p)$. The vector meson propagator $G_\omega(m)$ is given by

$$G_V(m) = \frac{1}{m^2 - m_V^2 + i m_V \Gamma_V(m)}, \tag{1}$$

where V stands for ρ^0, ω and ϕ mesons. For these mesons, we have values for their resonance masses and total widths [9]: $m_{V(\equiv\rho^0)} \simeq 768$ MeV, $\Gamma_{V(\equiv\rho^0)} \simeq 151$ MeV; $m_{V(\equiv\omega)} \simeq 782$ MeV, $\Gamma_{V(\equiv\omega)} \simeq 8.43$ MeV; and $m_{V(\equiv\phi)} \simeq 1020$ MeV, $\Gamma_{V(\equiv\phi)} \simeq 4.43$ MeV. The data taken at ELSA [8] show the peak at $\sim$780 MeV in the $\pi^0\gamma$ invariant mass distribution spectrum. Around this mass, the propagators for both ρ^0 and ω mesons behave as $G_V(m \approx 782\ \text{MeV}) \sim \frac{-i}{m_V\Gamma_V}(V \equiv \rho^0, \omega)$, whereas $G_\phi(m)$ goes as $G_\phi(m \approx 782\ \text{MeV}) \sim \frac{1}{m^2 - m_\phi^2}$. The decay widths for ρ^0, ω, and ϕ mesons in the $\pi^0\gamma$ branch (according to the Ref. [9]) are $\Gamma(768)_{\rho^0\to\pi^0\gamma} \approx 0.12$ MeV, $\Gamma(782)_{\omega\to\pi^0\gamma} \approx 0.72$ MeV, and $\Gamma(1020)_{\phi\to\pi^0\gamma} \approx 0.006$ MeV. In fact, $\Gamma_{\rho^0\to\pi^0\gamma}(m)$ is negligibly larger than 0.12 MeV and $\Gamma_{\phi\to\pi^0\gamma}(m)$ could be much less than 0.006 MeV at $m \approx 782$ MeV. Therefore, at 1.5 GeV the ratios $\frac{\sigma_t(\gamma p\to\omega p)}{\sigma_t(\gamma p\to\phi p)} \simeq 38.29$, $|\frac{G_\omega(m\approx782)}{G_\phi(m\approx782)}|^2 \sim 4.2\times10^3$, and $\frac{\Gamma(m\approx782)_{\omega\to\pi^0\gamma}}{\Gamma(m\approx782)_{\phi\to\pi^0\gamma}} > 120$ show that one can safely ignore the contribution to the cross section originating from the ϕ meson of mass around 782 MeV. For ρ^0 and ω mesons, these data show $\frac{\sigma_t(\gamma p\to\omega p)}{\sigma_t(\gamma p\to\rho^0 p)} \approx 0.28$, $|\frac{G_\omega(m\approx782)}{G_{\rho^0}(m\approx782)}|^2 \sim 3.1\times10^2$, and $\frac{\Gamma(m=782)_{\omega\to\pi^0\gamma}}{\Gamma(m=782)_{\rho^0\to\pi^0\gamma}} \approx 6$. Therefore, this analysis illustrates qualitatively that the contribution to the $\pi^0\gamma$ emission from the ω meson decay is a factor of about 521 times larger than that originating from the ρ^0 meson decay. Similar analysis shows this factor to be about 10^3 at E_γ equal to 1.2 GeV.

There were two aspects in the experiment (done at ELSA [8]) to be mentioned. One aspect in this measurement was

 ©2008 The American Physical Society

the γ beam of wide energy spread (0.64–2.53 GeV), since it was the tagged photon produced by the bremsstrahlung radiation of the 2.8 GeV electron on the Pb target. This is unlike in conventional experiments where the beam energy is taken to be almost monoenergetic. In fact, the measured $\pi^0\gamma$ invariant mass distribution spectrum has been reported for a definite ω meson momentum bin instead of a particular incident energy. Another aspect of this experimental setup was the large width in the detecting system (55 MeV), which is about 6.5 times larger than the width of the ω meson [i.e., $\Gamma_\omega(m = 782\ \text{MeV}) = 8.43$ MeV in the free state] produced in the γp reaction. Therefore, the measured $\pi^0\gamma$ invariant mass distribution spectrum showing its width of about 55 MeV can be attributed to the width of the detector resolution. To compare the calculated results with the data, I incorporate these two aspects in the formalism presented in Sec. II. The results of this study are discussed in Sec. III, and conclusions are presented in Sec. IV.

II. FORMALISM

The formalism for the $\pi^0\gamma$ emission in the γp reaction, as mentioned earlier, consists of the production, propagation, and the decay of the ω meson produced in the intermediate state (i.e., $\gamma p \to \omega p'; \omega \to \pi^0\gamma'$). The primes on p and γ are used at present to distinguish them from the initial state particles and will be dropped afterward for convenience. The T matrix T_{fi} for this process can be written as

$$T_{\text{fi}} = (\pi^0, \gamma'|\Gamma_{\omega\pi\gamma}|\omega)G_\omega(m)F(\gamma p \to \omega p'), \tag{2}$$

where $G_\omega(m)$ denotes the propagator for the ω meson. $(\pi^0\gamma'|\Gamma_{\omega\pi\gamma}|\omega)$ is the matrix element for $\omega \to \pi^0\gamma'$ resulting from intrinsic coordinates. It is governed by the Lagrangian density [13]

$$\mathcal{L}_{\omega\pi^0\gamma} = \frac{f_{\omega\pi\gamma}}{m_\pi}\epsilon_{\mu\nu\rho\sigma}\partial^\mu A^\nu \pi^0 \partial^\rho \omega^\sigma, \tag{3}$$

where A appearing in this equation represents the photon field. $f_{\omega\pi\gamma}$ is the constant for the $\omega\pi\gamma$ coupling and is equal to 0.095, as extracted from the width of $\omega \to \pi^0\gamma$ [9].

In Eq. (2), $F(\gamma p \to \omega p')$ describes the production mechanism for the ω meson in the γp reaction. It is given by

$$F(\gamma p \to \omega p') = -4\pi E_\omega \left[\frac{1}{E_\omega} + \frac{1}{E_{p'}}\right] \times \langle \omega, p'|f_{\gamma p\to\omega p'}(0)|\gamma, p\rangle, \tag{4}$$

where $f_{\gamma p\to\omega p'}(0)$ is the forward amplitude for the $\gamma p \to \omega p'$ reaction.

The differential cross section for this reaction can be written as

$$d\sigma = \frac{1}{2E_\gamma}(2\pi)^4\delta^4(k_i - k_f)\langle|T_{\text{fi}}|^2\rangle \frac{m_p}{E_{p'}}\frac{d^3\mathbf{k}_{p'}}{(2\pi)^3} \times \frac{1}{2E_{\pi^0}}\frac{d^3\mathbf{k}_{\pi^0}}{(2\pi)^3}\frac{1}{2E_{\gamma'}}\frac{d^3\mathbf{k}_{\gamma'}}{(2\pi)^3}. \tag{5}$$

The angular brackets around the T_{fi} matrix indicates the average over the polarization and spin in the initial state and the summation over the polarization and spin in the final state. Since the π^0 and γ bosons in the final state are considered to originate from the decay of the ω meson, this expression can be worked out in terms of the ω meson mass m (i.e., the $\pi^0\gamma'$ invariant mass) as

$$\frac{d\sigma(m, E_\gamma)}{dm} = \int d\Omega_\omega [KF]\Gamma_{\omega\to\pi^0\gamma'}(m) \times |G_\omega(m)|^2|F(\gamma p \to \omega p')|^2, \tag{6}$$

where $d\Omega_\omega$ is the infinitesimal solid angle subtended by the ω meson momentum $\mathbf{k}_\omega(= \mathbf{k}_{\pi^0} + \mathbf{k}_{\gamma'})$. $\Gamma_{\omega\to\pi^0\gamma'}(m)$ denotes the width for the ω meson of mass m decaying at rest into the $\pi^0\gamma$ channel [later expressed in Eq. (14)]. KF represents the kinematical factor for this reaction, which is given by

$$[KF] = \frac{3\pi^3}{(2\pi)^6}\frac{k_\omega^2 m_p m^2}{k_\gamma|k_\omega(E_\gamma + m_p) - \mathbf{k}_\gamma \cdot \hat{\mathbf{k}}_\omega E_\omega|}. \tag{7}$$

Equation (6) illustrates the differential cross section for the ω meson mass distribution from fixed beam (γ) energy E_γ. But the measurement was done by the CBELSA/TAPS Collaboration [8], as mentioned earlier, using a range of incident γ energies instead of fixed beam energy. We can incorporate this in our calculation by modulating the cross section in Eq. (6) with the beam profile function $W(E_\gamma)$ [14], that is,

$$\frac{d\sigma(m)}{dm} = \int_{E_\gamma^{mn}}^{E_\gamma^{mx}} dE_\gamma W(E_\gamma)\frac{d\sigma(m, E_\gamma)}{dm}. \tag{8}$$

E_γ^{mn} and E_γ^{mx} are equal to 0.64 and 2.53 GeV, respectively, as mentioned in Ref. [8]. The profile function $W(E_\gamma)$ for the γ beam, originating from bremsstrahlung radiation of the electron, varies as $W(E_\gamma) \propto \frac{1}{E_\gamma}$ [14].

The calculated cross section from Eq. (8) cannot reproduce the measured distribution, since the detecting system in the experimental setup (as mentioned earlier) had large resolution width (i.e., 55 MeV) [8]. This issue is incorporated in the formalism by folding the differential cross section in Eq. (8) with a Gaussian function $R(m, m')$:

$$\frac{d\sigma(m)}{dm} = \int dm' R(m, m')\frac{d\sigma(m')}{dm'}. \tag{9}$$

The function $R(m, m')$ accounts for the resolution (or response) of the detector. The expression for it [15] is

$$R(m, m') = \frac{1}{\sigma\sqrt{2\pi}}e^{-\frac{(m-m')^2}{2\sigma^2}}. \tag{10}$$

Here, σ is related to the full width at the half-maxima (FWHM) of this function as FWHM $= 2.35\sigma$. We take the value for FWHM equal to 55 MeV, so that the function $R(m, m')$ can describe properly the resolution for the detector used at ELSA [8].

III. RESULTS AND DISCUSSION

The amplitude for the $\gamma p \to \omega p$ reaction [i.e., $f_{\gamma p\to\omega p}(0)$ needed in Eq. (4)] is related to the four-momentum q^2 transfer

distribution $d\sigma(\gamma p \to \omega p)/dq^2$ [16] as

$$|f_{\gamma p\to\omega p}(q^2)|^2 = \frac{k_\gamma^2}{\pi}\frac{d\sigma}{dq^2}(\gamma p \to \omega p). \tag{11}$$

Therefore, the energy-dependent values for $|f_{\gamma p\to\omega p}(0)|^2$ [required to calculate the cross sections in Eqs. (8) and (9)] can be extracted from the four-momentum transfer distribution $d\sigma(\gamma p \to \omega p)/dq^2$. In fact, the forward $d\sigma(\gamma p \to \omega p)/dq^2$ is obtained by extrapolating the measured $d\sigma(\gamma p \to \omega p)/dq^2$ to $q^2 = 0$ for $E_\gamma \geqslant 1.6$ GeV [16,17]. It should be mentioned that in the present study the ω meson is dominantly produced at lower energy (i.e., $E_\gamma \leqslant 1.6$ GeV) in the γp reaction. Recently, the experiment had been carried out on the low-energy $\gamma p \to \omega p$ reaction with the SAPHIR detector at ELSA [11]. In this measurement, Barth *et al.* [11] have reported the measured $d\sigma(\gamma p \to \omega p)/dq^2$ vs $|q^2 - q^2_{\rm min}|$ (with $q^2_{\rm min}$ defined in Refs. [16,18]) in the energy region $E_\gamma = 1.1$–2.6 GeV. In addition, they have also shown that the measured $d\sigma(\gamma p \to \omega p)/dq^2$ behaves as $\sim \exp[b(q^2 - q^2_{\rm min})]$ in the low four-momentum q^2 transfer region. Since this energy region is well in accordance with the study here, I extract $|f_{\gamma p\to\omega p}(0)|^2$ from the SAPHIR data and use it in our calculation.

The ω meson propagator $G_\omega(m)$ in Eq. (6) can be described by Eq. (1). The total width $\Gamma_\omega(m)$ appearing in it is composed of widths from the ω meson decaying into various

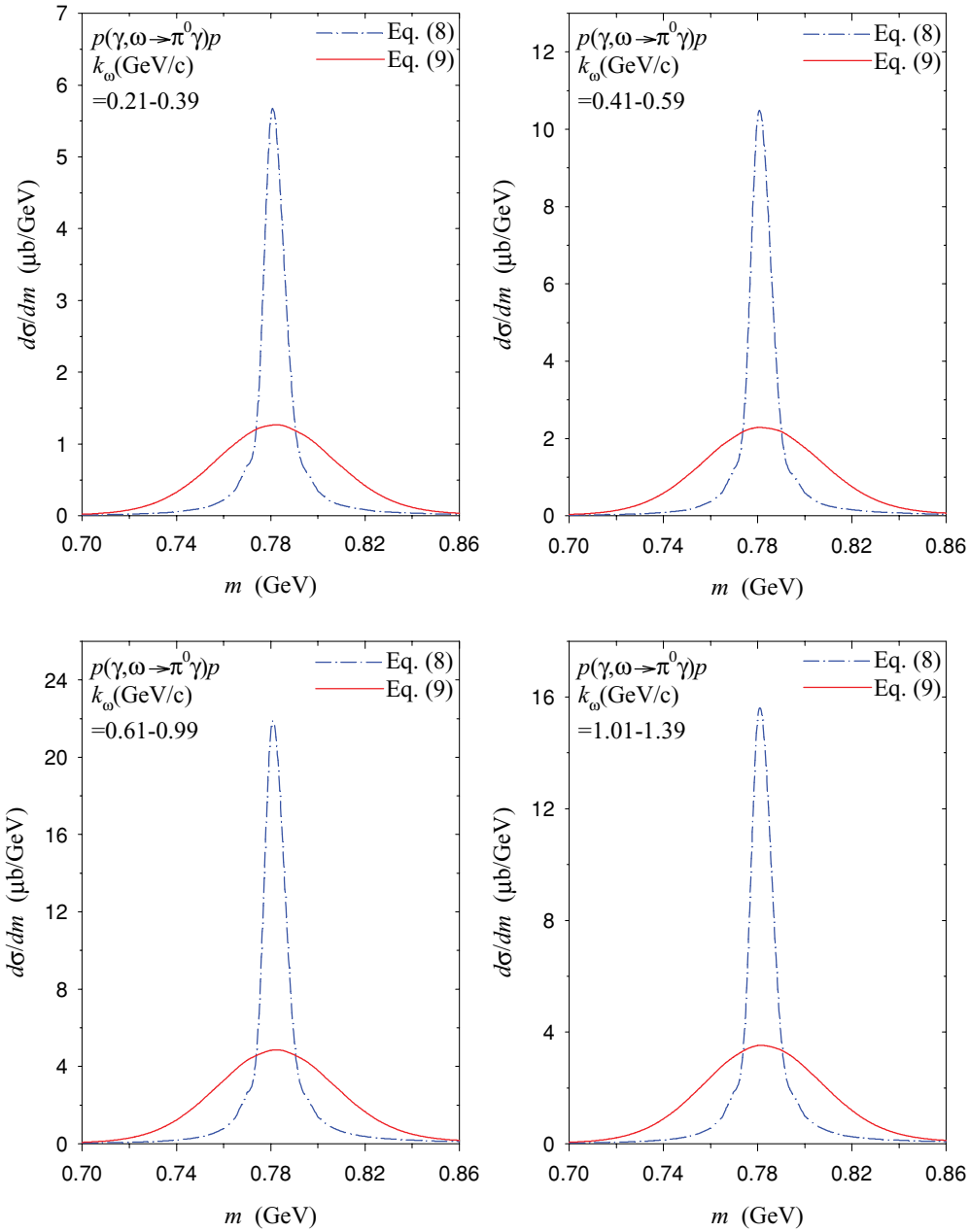

FIG. 1. (Color online) The ω meson mass distribution spectra for various ω meson momentum bins. The dash-dot curves correspond to the calculated results from Eq. (8), whereas the solid curves arise from Eq. (9) (see text).

channels [9]:

$$\Gamma_\omega \approx \Gamma_{\omega\to\pi^+\pi^-\pi^0}(88.8\%) + \Gamma_{\omega\to\pi^0\gamma}(8.5\%) + \Gamma_{\omega\to\pi^+\pi^-}(2.21\%) + \Gamma_{\omega\to l^+l^-}(\sim 10^{-4}\%). \quad (12)$$

One can ignore here widths from the leptonic decay ($\Gamma_{\omega\to l^+l^-}$), since they are insignificant. The typical magnitudes for them are of the order of keV or less, whereas the widths for the ω meson decaying into other channels in Eq. (12) are within the range of 100 keV to 10 MeV.

$\Gamma_{\omega\to\pi^+\pi^-\pi^0}(m)$ in Eq. (12) represents the width for the $\omega \to \pi^+\pi^-\pi^0$ channel. We use the form for it as derived by Sakurai [19]:

$$\Gamma_{\omega\to\pi^+\pi^-\pi^0}(m) = \Gamma_{\omega\to\pi^+\pi^-\pi^0}(m_\omega)\frac{m}{m_\omega}\frac{(m-3m_\pi)^4}{(m_\omega-3m_\pi)^4}\frac{U(m)}{U(m_\omega)}, \quad (13)$$

with $\Gamma_{\omega\to\pi^+\pi^-\pi^0}(m_\omega = 782\ \text{MeV}) \approx 7.49$ MeV. $U(m) \to 1$ as $m \to 3m_\pi$ and $U(m) \to 1.6$ as $m \to 787$ MeV. I have also taken $U(m)$ equal to 1.6 for $m > 787$ MeV.

The width $\Gamma_{\omega\to\pi^0\gamma}(m)$ in Eq. (12) arises from $\omega \to \pi^0\gamma$ channel. By using the Lagrangian density $\mathcal{L}_{\omega\pi\gamma}$ given in

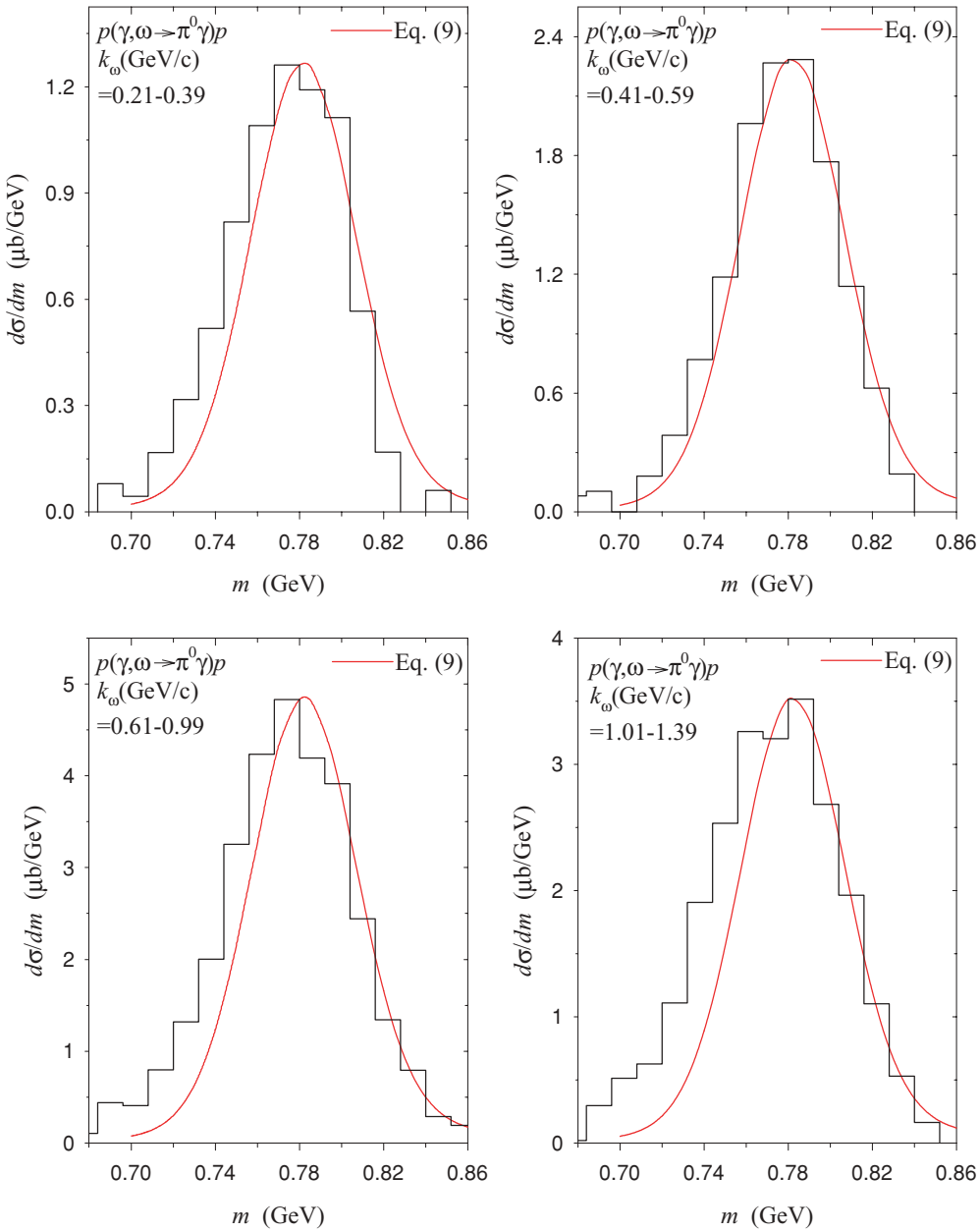

FIG. 2. (Color online) The calculated ω meson mass distribution spectra for various ω meson momentum bins compared with the data (see text). The solid curves correspond to the calculated results from Eq. (9). The histograms represent the measured counts for the $\pi^0\gamma$ invariant mass distribution spectra [8], normalized to the respective calculated peaks.

Eq. (3), it is evaluated as

$$\Gamma_{\omega\to\pi^0\gamma}(m) = \Gamma_{\omega\to\pi^0\gamma}(m_\omega)\left[\frac{k(m)}{k(m_\omega)}\right]^3, \qquad (14)$$

with $\Gamma_{\omega\to\pi^0\gamma}(m_\omega) \approx 0.72$ MeV at $m_\omega = 782$ MeV. Here $k(m)$ denotes the momentum of the pion originating from the ω meson of mass m decaying at rest.

In Eq. (12), $\Gamma_{\omega\to\pi^+\pi^-}(m)$ denotes the width for the ω meson decaying into the $\pi^+\pi^-$ channel. This channel arises from the small pure isovector ρ meson component present in the physical ω meson [1]. By using the Lagrangian density $\mathcal{L}_{\omega\pi\pi} = f_{\omega\pi\pi}(\vec{\pi}\times\partial_\mu\vec{\pi})\cdot\omega^\mu$, the width for this channel is worked out as

$$\Gamma_{\omega\to\pi^+\pi^-}(m) = \Gamma_{\omega\to\pi^+\pi^-}(m_\omega)\frac{m_\omega}{m}\left[\frac{k(m)}{k(m_\omega)}\right]^3, \qquad (15)$$

where $k(m)$ represents the pion momentum in the $\pi^+\pi^-$ center-of-mass system. The value for $\Gamma_{\omega\to\pi^+\pi^-}(m_\omega = 782$ MeV), according to Ref. [9], is approximately equal to 0.19 MeV.

We can now calculate the cross sections for the ω meson mass distribution in the γ-induced reaction on a proton target. The calculated results have been compared with the measured $\pi^0\gamma$ invariant mass distribution spectra in the $p(\gamma,\pi^0\gamma)p$ reaction, since the π^0 and γ in the final state (as mentioned earlier) are assumed to originate from the decay of the ω meson produced in the intermediate state. The measured $\pi^0\gamma$ invariant mass distribution spectra have been reported in Ref. [8] for four ω meson momentum bins: (i) $0.2 < k_\omega$ (GeV/c) < 0.4, (ii) $0.4 < k_\omega$ (GeV/c) < 0.6, (iii) $0.6 < k_\omega$ (GeV/c) < 1, and (iv) $1 < k_\omega$ (GeV/c) < 1.4. Therefore, I have calculated cross section for (i) $k_\omega = 0.21$–0.39 GeV/c, (ii) $k_\omega = 0.41$–0.59 GeV/c, (iii) $k_\omega = 0.61$–0.99 GeV/c, and (iv) $k_\omega = 1.01$–1.39 GeV/c.

The ω meson mass distribution spectra calculated using Eq. (8) are presented in Fig. 1 by the dash-dot curves. The sharp peak at a mass of around 780 MeV and a width of about 8.43 MeV, appearing in these curves, are the characteristic features for the ω meson produced in the free state. The solid curves in this figure illustrate the ω meson mass distribution spectra calculated using Eq. (9). These curves arise from the folding of the calculated cross section given in Eq. (8) with the detector resolution function $R(m, m')$ in Eq. (10). Therefore, the incorporation of the detector resolution function in the calculated cross section, as shown in this figure, has widened all spectra and, simultaneously, reduces the cross section at the peak. The enhancement in the width from ~8.43 MeV (dash-dot curves) to ~55 MeV (solid curves) occurs because of the width appearing in the detector resolution function $R(m, m')$ [see Eq. (10)].

In Fig. 2, I compare the calculated results from Eq. (9) with the measured $\pi^0\gamma$ invariant mass distribution spectra for all ω meson momentum bins. This figure shows that the calculated ω meson mass distribution folded duly with the detector resolution function, as described here, reproduces the data very well for all bins of the ω meson momentum.

IV. CONCLUSION

The differential cross section for the $\pi^0\gamma$ invariant mass distribution in the γp reaction has been calculated. The analysis shows that the $\pi^0\gamma$ appearing in the final state is occurring dominantly from the decay of the ω meson produced in the intermediate state. The calculated results showing a sharp and narrow peak characterize the production of the ω meson in the free state. The incorporation of the Gaussian function (to describe the detector resolution) in the calculation broadens the ω meson mass distribution spectrum, which is in accordance with the data.

ACKNOWLEDGMENTS

I gratefully acknowledge L. M. Pant for making me aware of the measurement of the ω meson mass distribution at ELSA. The discussion with D. R. Chakrabarty on the detector resolution is highly appreciated. The communication made with E. Oset regarding the beam profile function is very helpful. I acknowledge D. Trnka and V. Metag for sending the data. I thank A. K. Mohanty, R. K. Choudhury, and S. Kailas for their support.

[1] T. H. Bauer, R. D. Spital, D. R. Yennie, and F. M. Pipkin, Rev. Mod. Phys. **50**, 261 (1978); D. R. Yennie, *ibid.* **47**, 311 (1975); H. B. O'Connell, B. C. Pearce, A. W. Thomas, and A. G. Williams, Prog. Part. Nucl. Phys. **39**, 201 (1997).

[2] W. Peters, M. Post, H. Lenske, S. Leupold, and U. Mosel, Nucl. Phys. **A632**, 109 (1998); M. Post, S. Leupold, and U. Mosel, *ibid.* **A689**, 753 (2001).

[3] M. F. M. Lutz, G. Wolf, and B. Friman, Nucl. Phys. **A706**, 431 (2002); B. Friman, Acta Phys. Pol. B **29**, 3195 (1998).

[4] E. Oset *et al.*, Pramana **66**, 731 (2006).

[5] G. M. Huber *et al.*, Phys. Rev. C **68**, 065202 (2003); G. M. Huber, G. J. Lolos, and Z. Papandreou, Phys. Rev. Lett. **80**, 5285 (1998); G. J. Lolos *et al.*, *ibid.* **80**, 241 (1998).

[6] S. Das, Nucl. Phys. **A781**, 509 (2007); Phys. Rev. C **72**, 064619 (2005); V. L. Eletsky and B. L. Ioffe, Phys. Rev. Lett. **78**, 1010 (1997); V. L. Eletsky, B. L. Ioffe, and J. I. Kapusta, Eur. Phys. J. **A3**, 381 (1998); L. A. Kondratyuk, A. Sibirtsev, W. Cassing, Y. S. Golubeva, and M. Effenberger, Phys. Rev. C **58**, 1078 (1998); M. Effenberger, E. L. Bratkovskaya, and U. Mosel, Phys. Rev. C **60**, 044614 (1999); Th. Weidmann, E. L. Bratkovskaya, W. Cassing, and U. Mosel, *ibid.* **59**, 919 (1999); M. Effenberger, E. L. Bratkovskaya, W. Cassing, and U. Mosel, *ibid.* **60**, 027601 (1999); Ye. S. Golubeva, L. A. Kondratyuk, and W. Cassing, Nucl. Phys. **A625**, 832 (1997); D. Cabrera and M. J. Vicente Vacas, Phys. Rev. C **67**, 045203 (2003); D. Cabrera, L. Roca, E. Oset, H. Toki, and M. J. Vicente Vacas, Nucl. Phys. **A733**, 130 (2004); V. K. Magas, L. Roca, and E. Oset, Phys. Rev. C **71**, 065202 (2005).

[7] R. Muto *et al.*, J. Phys. G: Nucl. Part. Phys. **30**, S1023 (2004); H. En'yo *et al.*, KEK Experiment E325; S. Yokkaichi *et al.* (KEK-PS E325 Collaboration), Nucl. Phys. **A638**, 435c (1998); Report Nos. INS-ES-134 and INS-ES-144, Report No. LBL-91 revised, UC-414, 1994, p. 108 (unpublished); K. Maruyama, in *Proceedings of the 25th*

International Symposium on Nuclear and Particle Physics with High Intensity Proton Accelerators (World Scientific, Singapore, 1998); Nucl. Phys. **A629**, 351c (1998); D. Heddle and B. M. Preedom, CEBAF Proposal No. PR 89-001 (unpublished); P. Y. Bertin, M. Kossov, and B. M. Preedom, CEBAF Proposal No. PR 94-002 (unpublished); W. Koenig (HADE Collaboration), in *Proceedings of the Workshop on Dilepton Production in Relativistic Heavy Ion Collisions*, edited by H. Bokemeyer (GSI, Darmstadt, 1994), p. 225; HADE Proposal, R. Schicker *et al*. Nucl. Instrum. Methods **A380**, 586 (1996); J. Friese, Prog. Part. Nucl. Phys. **42**, 235 (1999); M. Fujiwara, Prog. Part. Nucl. Phys. **50**, 487 (2003).

[8] D. Trnka *et al*. (CBELSA/TAPS Collaboration), Phys. Rev. Lett. **94**, 192303 (2005).

[9] Particle Data Group, Phys. Rev. D **54**, 331 (1996); **54**, 334 (1996); **54**, 341 (1996).

[10] Aachen-Berlin-Bonn-Hamburg-Heidelberg-München Collaboration, Phys. Rev. **175**, 1669 (1968).

[11] J. Barth *et al*., Eur. Phys. J. A **18**, 117 (2003).

[12] J. Barth *et al*., Eur. Phys. J. A **17**, 269 (2003).

[13] J. A. Gómez Tejedor and E. Oset, Nucl. Phys. **A600**, 413 (1996); G. I. Lykasov, W. Cassing, A. Sibirtsev, and M. V. Rzjanin, Eur. Phys. J. A **6**, 71 (1999); M. Gourdin, in *Meson Resonance and Related Electromagnetic Phenomena*, edited by R. H. Dalitz and A. Zichichi (Editrice Compositori, Bologna, Italy, 1972) p. 219.

[14] M. Kaskulov, E. Hernandez, and E. Oset, nucl-th/0610067; Eur. Phys. J. A **31**, 245 (2007).

[15] G. F. Knoll, *Radiation Detection and Measurement* (John Wiley & Sons, New York, 1989), p. 116.

[16] A. Sibirtsev, H.-W. Hammer, U.-G. Meißner, and A. W. Thomas, Eur. Phys. J. A **29**, 209 (2006).

[17] A. Sibirtsev, K. Tsushima, and S. Krewald, nucl-th/0202083; Phys. Rev. C **67**, 055201 (2003).

[18] W. J. Schwille, F. J. Klein, F. Klein, and J. Barth (private communication); Particle Data Group, Phys. Lett. **B667**, 340 (2008).

[19] J. J. Sakurai, Phys. Rev. Lett. **8**, 300 (1962).